Mbarki et al., J Material Sci Eng 2016, 5:4
DOI: 10.4172/2169-0022.1000264

Journal of Material Sciences & Engineering

Research Article Open Access

Investigation of the Flexoelectric Coupling Effect on the 180° Domain Wall Structure and Interaction with Defects

Mbarki R[1]*, Borvayeh L[2] and Sabati M[3,4]

[1]Department of Mechanical Engineering, The Australian College of Kuwait, Meshraf, Kuwait
[2]Department of Mathematics, The Australian College of Kuwait, Meshraf, Kuwait
[3]Department of Electrical Engineering, The Australian College of Kuwait, Meshraf, Kuwait
[4]The Dr. John T. Macdonald Foundation Biomedical Nanotechnology Institute, Department of Radiology, University of Miami, USA

Abstract

A new theory for 180° domain wall in ferroelectric perovskite material is presented in this work. The effect of flexoelectric coupling on the domain structure is analyzed. We show that the 180° domain wall has a mixed character of Ising and Bloch type wall and that the polarization perpendicular to the domain wall is not zero though it is very small compared to the spontaneous polarization in the case of tetragonal Barium Titanate. Finally, we present the effect of the new finding on the domain wall interaction with defects in the material.

Keywords: Flexoelectric; Coupling; Dielectric; Piezoelectric; Ferroelectric materials

Introduction

Perovskite ferroelectric materials are known for a superior dielectric and piezoelectric response. They have attracted attention for applications in technologies like capacitors, microelectromechanical systems (MEMS), nonvolatile memories as well as nonlinear optical applications. Ferroelectric materials usually display domains consisting of regions that are either ordered along the same axis but with opposite polarity also called 180° domain walls (Figure 1) or along different orthogonal axis. The existence of these domain walls has a significant influence on the material properties. The measured material properties have two contributions, an intrinsic response which is the property of a single domain material and the extrinsic response which consists of domain wall contribution. For example, it has been shown that for Lead zirconate titanate (PZT) at composition near the morphotropic phase boundary, the domain wall contribution represents more than half of the dielectric and piezoelectric response at room temperature [1]. Ghosh et al. [2] studied experimentally the effect of domain wall motion on the piezoelectric properties of ferroelectric material. They showed that the motion of the domain wall is responsible for the high permittivity and piezoelectric coefficient in Barium Titanate.

The 180° domain wall formed in ferroelectric materials is generally assumed to be an Ising type domain. However, it can generally be either an Ising or a Bloch type domain. In the Ising type, the polarization tends to switch sign by decreasing in magnitude in the plane of the domain wall. While in the Bloch type, the polarization tends to switch sign by rotating outside the plane of the wall and maintaining a constant magnitude (Figure 2). A mixture of Ising and Bloch types is possible where the polarization changes sign by rotating outside of the wall plane and decreasing in magnitude as it gets closer to the wall.

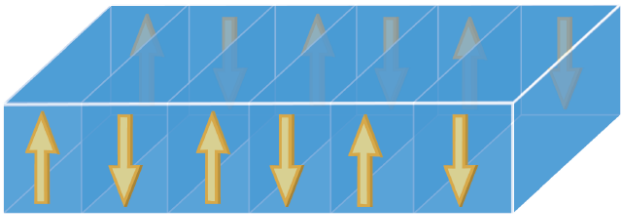

Figure 1: Example of 180° domain wall.

Huang et al. [3] investigated the type of the domain that can form in the tetragonal phase of a ferroelectric perovskite. They showed theoretically that upon cooling material, the domain wall can switch from an Ising type to a Bloch type. Lee et al. [4] performed an ab *initio* calculation and showed that the 180° domain wall in ferroelectric perovskite shows a mixed character.

Ferroelectric domain walls have been studied by many researchers [5-9]. The work started by the Landau Devonshire theory where the Gibbs free energy density is expanded to sixth power of the polarization including a polarization gradient term. However, this formulation did not take into consideration the electromechanical coupling between strain and polarization. Further expansion of the Gibbs free energy is required to take into consideration the ferroelastic nature of this material. Later studies included this coupling e.g., Huang et al. [3] and Cao et al. [9].

In the last decade, ferroelectric materials have also been exploited and studied at small scales. Researchers have shown that at the nanoscale flexoelectricity becomes very important especially for perovskite materials which are known for their high flexoelectric coefficient [10,11]. Recent work by Yudin et al. [8] presented a new formulation for the domain wall energy in which, they included the flexoelectric coupling. They assumed that the polarization in the plane

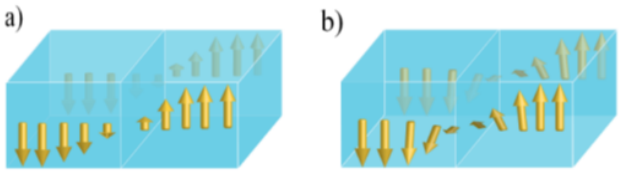

Figure 2: Different types of domain wall: a) Ising type b) Bloch type.

***Corresponding author:** Mbarki R, Department of Mechanical Engineering, The Australian College of Kuwait, Meshraf, Kuwait, Tel: 96525376111; E-mail: rmbarki@uh.edu

Received May 28, 2016; **Accepted** June 14, 2016; **Published** June 24, 2016

Citation: Mbarki R, Borvayeh L, Sabati M (2016) Investigation of the Flexoelectric Coupling Effect on the 180° Domain Wall Structure and Interaction with Defects. J Material Sci Eng 5: 264. doi:10.4172/2169-0022.1000264

of the domain wall is not zero and that the polarization perpendicular to the wall vanishes because of the depoling field across the wall. Such assumption can reduce the accuracy of the calculation especially with the existence of a high strain gradient across the domain which induces polarization in the perpendicular direction due to the flexoelectric coupling. In this work, we develop a theory for perovskite ferroelectrics in the tetragonal phase. We present numerical results for 180° domain wall in Barium Titanate material with a random defects distribution. We show that the flexoelectric effect transforms the 180° domain wall to a mixture of Bloch and Ising type. Then, we show the effect of the flexoelectricity on the defects interaction with the domain wall.

Model Formulation

Let us consider a thin film of perovskite material with a 4 *mm* symmetry in the tetragonal phase occupying a volume in the space (Figure 3). [x_1; x_2; x_3] is the cubic crystallographic direction. The 180° domain wall lies in the (100) plane. Two platinum electrodes are fixed on each surface of the thin film. Upon cooling to temperature below the Curie temperature T_c, the material tends to reduce its total free energy by creating the domain structure. The creation of the domain structure is accompanied by the distortion of the unit cell which induces a spontaneous strain ε^s and the generation of spontaneous polarization P^s. Far away from the domain wall, the strain and the polarization are defined by these vectors. Near the domain wall, it is reasonable to assume that the polarization varies significantly although the elastic strain remains small. The equilibrium state is defined by the spontaneous polarization P^s, the spontaneous strain ε^s and the spontaneous strain gradient η^s. The polarization gradient is zero at equilibrium. The free energy density can be expanded around the equilibrium state

$$W(\mathrm{P},\varepsilon,\nabla\mathrm{P},\nabla\varepsilon)=\frac{1}{2}\nabla P.\frac{\partial^2 W}{\partial(\nabla P)^2}\nabla P+\frac{1}{2}(\nabla\varepsilon-\eta^s).\frac{\partial^2 \mathrm{W}}{\partial(\nabla\varepsilon)^2}(\nabla\varepsilon-\eta^s)+\frac{1}{2}(\varepsilon-\varepsilon^s).\frac{\partial^2 W}{\partial\varepsilon^2}(\varepsilon-\varepsilon^s)+\frac{1}{2}\nabla P.\frac{\partial^2 W}{\partial\nabla P\partial\varepsilon}(\varepsilon-\varepsilon^s)+W_{\mathrm{L}}(Ps,\varepsilon^s,\mathrm{o},\eta^s) \quad (1)$$

where $W_{\mathrm{L}}(\mathrm{P}, \varepsilon^s, 0, \eta^s)$ is the Landau free energy given by the following expression

$$W_L(P)=\frac{a_1}{2}(P_1^2+P_2^2)+\frac{a_2}{4}(P_1^4+P_2^4)+\frac{a_3}{2}(P_1^2+P_2^2)+\frac{a_4}{6}(P_1^6+P_2^6)+\frac{a_5}{4}(P_1^4+P_2^4) \quad (2)$$

During the phase transition from cubic to tetragonal phase, the free energy given by equation 1 can describe the limit transition. If we match Equation 1 with the free energy in the cubic phase, it is possible to determine an expressions for the spontaneous strain and the spontaneous strain gradient. The free energy density in the cubic phase *Wc* is given by the following expression

$$W_c(P,\varepsilon,\nabla\mathrm{P},\nabla\varepsilon)=W_L(P)+\frac{1}{2}(\varepsilon-\varepsilon^s).C(\varepsilon-\varepsilon^s)+\frac{1}{2}(\nabla\varepsilon-\eta^s).G(\nabla\varepsilon-\eta^s)+\frac{1}{2}\nabla P.a_0\nabla P+\frac{1}{2}\nabla P.d(\varepsilon-\varepsilon^s)+Pf\nabla\varepsilon \quad (3)$$

where *C* is the elastic tensor given by the following expression

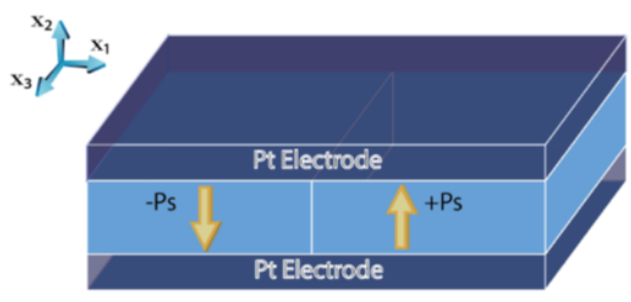

Figure 3: 180° domain wall with two platinum electrodes on each side.

$$C_{ijkl}=\frac{\partial^2 W}{\partial\varepsilon_{ij}\partial\varepsilon_{kl}} \quad (4)$$

d is the fourth order tensor introduced by Mindlin in the polarization gradient theory [12]

$$d_{ijkl}=\frac{\partial^2 W}{\partial P_{i,j}\partial\varepsilon_{kl}} \quad (5)$$

and *f* is the fourth order flexoelectric tensor

$$f_{ijkl}=\frac{\partial^2 W}{\partial P_l\,\partial\varepsilon_{ij,k}} \quad (6)$$

It is obvious that the spontaneous polarization P^s, the spontaneous strain ε^s and the spontaneous strain gradient η^s are function of the polarization. In order to determine the expressions of these tensors, a matching between the equations 1 and 3 is necessary.

The term coupling the polarization and the strain in equation 1 is the piezoelectric tensor *e* given by the following expression

$$e=\frac{\partial^2 W}{\partial P\partial\varepsilon} \quad (7)$$

In the cubic phase, the material is not piezoelectric so there is no coupling between polarization and strain. However, at the transition limit between cubic and tetragonal phases, deriving the free energy in the cubic phase given by Equation (3) with respect to the polarization and the strain, we should be able to find an equivalent to this coupling.

$$e=\frac{\partial^2 W_c}{\partial P\partial\varepsilon}=-C\frac{d\varepsilon^s}{dP} \quad (8)$$

The integration of the equation 8 gives the following result

$$\varepsilon^s=\varepsilon^s(P^s)-S:e(P-P^s) \quad (9)$$

where $S = C^{-1}$ is the elastic compliance.

Same procedure used to determine the spontaneous strain gradient η^s gives the following result

$$\eta^s=-G^{-1}:f(P-P^s) \quad (10)$$

Equation 1 can be rewritten as follow:

$$W(P,\varepsilon,\nabla P,\nabla\varepsilon)=\frac{1}{2}(\varepsilon-\varepsilon^s).C(\varepsilon-\varepsilon^s)+\frac{1}{2}(\nabla\varepsilon-\eta^s).G(\nabla\varepsilon-\eta^s)+\frac{1}{2}\nabla P.a_0\nabla P+\frac{1}{2}\nabla P.d(\varepsilon-\varepsilon^s)+W_L(P) \quad (11)$$

The governing equations of polarization and strain evolution are obtained as the gradient flow associated with the Gibbs free energy. For further information on how to obtain these equations, the reader is advised to refer to Zhang et al. [13]:

$$\mu\frac{dP}{dt}=-\frac{\partial W}{\partial P}+\nabla.\left(\frac{\partial W}{\partial P\nabla}\right)-\nabla\phi \qquad \text{in}\,\Omega \quad (12)$$

$$v\frac{du}{dt}=\tilde{N}.\left(\frac{\partial W}{\partial\varepsilon}\right)-\nabla\nabla.\left(\frac{\partial W}{\partial\nabla\varepsilon}\right)=0 \qquad in\,\Omega \quad (13)$$

Subjected to the corresponding boundary conditions on $\partial\Omega$:

$$\frac{\partial W}{\partial\nabla P}.n=0 \qquad on\,\partial\Omega\ and \quad (14)$$

$$\left(\frac{\partial W}{\partial\varepsilon}-\nabla.\left(\frac{\partial W}{\partial\nabla\varepsilon}\right)\right).n=0 \qquad on\,\partial\Omega, \quad (15)$$

where *n* is the outward normal vector to the surface $\partial\Omega$, Φ is the electrostatic potential, μ and ν are respectively, the inverse of the polarization and strain mobility.

The 180° domain wall can be described as 1D problem where all the variables are function of one independent variable x_1. There are no assumptions on the polarization vector. The spontaneous polarization can be described by the following equations:

$$P_1^s = \frac{P_0}{2}(tanh(\frac{P_1 + P_2}{l}) + tanh(\frac{P_1 - P_2}{l}))$$
$$P_2^s = \frac{P_0}{2}(tanh(\frac{P_1 + P_2}{l}) - tanh(\frac{P_1 - P_2}{l})) \quad (16)$$

where P_0 is the magnitude of the spontaneous polarization at large distance from the domain wall, and l is a shape factor that controls how fast the spontaneous polarization changes across the domain wall. The component of the polarization P_2 is parallel to the domain wall and the component P_1 is normal to the wall. We consider two cases: the first case is a perovskite crystal without defects and the second case is a doped perovskite crystal with random oxygen vacancies. The electrostatic equation for the first case is the solution of the Poisson equation:

$$\nabla.(-\varepsilon_0 \nabla \Phi + P) = 0 \quad (17)$$

$$n.(-\varepsilon_0 \nabla \Phi + P) = 0 \quad (18)$$

In the presence of defects in crystal, the electrostatic potential Φ, the polarization P and the charge density ρ are related by the Maxwell equation

$$\nabla.(-\varepsilon_0 \nabla \Phi + P_{X\Omega}) = \rho X\Omega \quad (19)$$

where $X\Omega$ is a characteristic function

$$\times_{\Omega} = \begin{cases} 1, & if\ x \in \Omega \\ 0, & otherwise \end{cases} \quad (20)$$

The charge density at any point is

$$\rho = q(N_d^+ - n_c + n_v) \quad (21)$$

where q is the electron charge, N_d^+ is the density of ionized donors, n_c is the density of electron in conduction band and n_v is the density of holes in the valence band. N_d^+, n_c and n_v are given by the Fermi-Dirac Distribution for fermions:

$$n_c = \frac{N_c}{1 + e^{\beta(E_c - q\phi - \mu_{nc})}} \quad (22)$$

$$n_v = \frac{N_v}{1 + e^{\beta(-E_v + q\phi - \mu_{nv})}} \quad (23)$$

$$N_d^+ = N_d(1 - \frac{1}{1 + \frac{1}{2}e^{\beta(E_d - q\phi - (\mu_{N_d^0} - \mu_{N_d^+}))}}) \quad (24)$$

$\mu_{n_c}, \mu_{n_v}, \mu_{N_d^0}$ and $\mu_{N_d^+}$ are the electrochemical potentials. E_c is the energy at the bottom of the conduction band, E_v is the energy on the top of the valence band and E_d is the donors level and $\beta = (K_b T)^{-1}$.

The space charge evolution in Ω is given by:

$$\frac{dn_c}{dt} = k_1 N_d^0(1 - e^{\beta(\mu_{nc} + \mu_{N_d^+} - \mu_{N_d^0})}) + k_2 N_v(1 - e^{\beta(\mu_{nc} + \mu_{pv})}) + \nabla.(K_1 \nabla \mu_{n_c}) \quad (25)$$

$$\frac{dn_v}{dt} = k_3 N_d^+(1 - e^{\beta(\mu_{nc} - \mu_{N_d^+} + \mu_{N_d^0})}) + k_2 N_v(1 - e^{\beta(\mu_{nc} + \mu_{pv})}) + \nabla.(K_2 \nabla \mu_{n_c}) \quad (26)$$

$$\frac{dN_d^+}{dt} = k_1 N_d^0(1 - e^{\beta(\mu_{nc} + \mu_{N_d^+} - \mu_{N_d^0})}) - k_3 N_d^+(1 - e^{\beta(\mu_{nc} - \mu_{N_d^+} + \mu_{N_d^0})}) \quad (27)$$

$$N_d^0 = N_d - N_d^+ \quad (28)$$

With the corresponding boundary conditions:

$$K_1 \nabla \mu_{n_c}.n = -k_4(e^{\beta(\mu_{n_c} + \phi_e)} - 1) \quad on\ \partial\Omega \quad (29)$$

$$\nabla \mu_{n_v}.n = 0 \quad on\ \partial\Omega \quad (30)$$

Where k_1, k_2, k_3 are rate constants for the species interconversion reactions, K_1, K_2 are diffusion constants and Φ_e is the work function of the electrodes.

The expression of the spontaneous strain is

$$\begin{aligned} \varepsilon_{11}^s &= \alpha^t - 1 - (S_{11}e_{12} + S_{12}e_{22})(P_2 - P_2^s) \\ &= \alpha^t - 1 - K_{11}(P_2 - P_2^s) \\ \varepsilon_{22}^s &= \beta^t - 1 - (S_{12}e_{12} + S_{11}e_{22})(P_2 - P_2^s) \\ &= \beta^t - 1 - K_{22}(P_2 - P_2^s) \\ \varepsilon_{12}^s &= -S_{44}\, e_{61}(P_1 - P_1^s) \\ &= K_{12}(P_1 - P_1^s) \end{aligned} \quad (31)$$

where $\alpha^t = 0{:}9958$ and $\beta^t = 1{:}0067$ are the two stretch components for tetragonal distortion [14-16]. The equation 12 becomes

$$\begin{aligned} &\mu\frac{\partial P_1}{\partial t} = -a_1P_1 - a_2P_1^3 - a_3P_1P_2^3 - a_4P_1^5 - a_5P_1^3P_2^4 + (d_{11} - f_{11}(1 - \frac{\partial P_1^s}{\partial P_1}))\frac{\partial^2 u_1}{\partial x_1^2} \\ &+e_{12}\frac{\partial P_1^s}{\partial P_2}\frac{\partial u_1}{\partial x_1} - \frac{d\phi}{dx_1} + (K_{11}e_{12} + K_{22}e_{22} + f_{12}\Gamma_{12} + f_{11}\Gamma_{11})\frac{\partial P_1^s}{\partial P_2}(P_2 - P_2^s) \\ &-(K_{12}e_{61} + f_{11}\Gamma_{11} + f_{12}\Gamma_{12})(1 - \frac{\partial P_1^s}{\partial P_1})(P_1 - P_1^s) + e_{12}(1 - \alpha^t)\frac{\partial P_1^s}{\partial P_2} + a_0\frac{d_2P_1}{dx_1^2} \\ &+(d_{11}K_{11} + d_{12}K_{12} - 2d_{44}K_{12})(1 - \frac{\partial P_1^s}{\partial P_1})\frac{dP_2}{dx_1} \end{aligned} \quad (32)$$

$$\begin{aligned} &\mu\frac{\partial P_2}{\partial t} = -a_1P_2 - a_2P_2^3 - a_3P_2P_1^2 - a_4P_2^5 - a_5P_2^3P_1^4 + f_{11}\frac{\partial P_1^s}{\partial P_2}\frac{\partial^2 u_1}{\partial x_1^2} + a_0\frac{d^2P_2}{dx_1^2} \\ &-e_{12}(\frac{\partial u_1}{\partial x_1} + 1 - \alpha^t)(1 - \frac{\partial P_1^s}{\partial P_1}) - (K_{11}e_{12} + K_{22}e_{22})(1 - \frac{\partial P_1^s}{\partial P_1})(P_2 - P_2^s) \\ &-(f_{12}\Gamma_{12} + f_{11}\Gamma_{11})(1 - \frac{\partial P_1^s}{\partial P_1})(P_2 - P_2^s) + (K_{12}e_{61} + f_{11}\Gamma_{11} + f_{12}\Gamma_{12}\frac{\partial P_1^0}{\partial P_2}(P_1 - P_1^s) \\ &+(d_{11}K_{11} + d_{12}K_{12} - 2d_{44}K_{12})(1 - \frac{\partial P_1^s}{\partial P_1})P_{1,1} \end{aligned} \quad (33)$$

The equation 13 becomes:

$$v\frac{\partial u_1}{\partial t} = C_{11}\frac{\partial^2 u_1}{\partial x_1^2} + e_{12}(\frac{\partial P_2}{\partial x_1} - \frac{\partial P_2^s}{\partial x_1}) + d_{11}\frac{\partial^2 P_1}{\partial x_1^2} - G_{11}\frac{\partial^4 u_1}{\partial x_1^4} - f_{11}(\frac{\partial^2 P_1}{\partial x_1^2} - \frac{\partial^2 P_2^s}{\partial x_1^2}) \quad (34)$$

$$v\frac{\partial u_2}{\partial t} = e_{61}(\frac{\partial P_1}{\partial x_1} - \frac{\partial P_1^s}{\partial x_1}) - f_{44}(\frac{\partial^2 P_2}{\partial x_1^2} - \frac{\partial^2 P_2^s}{\partial x_1^2}) + d_{44}\frac{\partial^2 P_2}{\partial x_1^2} \quad (35)$$

The Boundary conditions become:

$$\frac{dP_1}{dx_1} + d_{11}\frac{du_1}{dx_1} + (d_{11}K_{11} + d_{12}K_{22})(P_2 - P_2^s) = d_{11}(\alpha^t - 1) \quad (36)$$

$$\frac{dP_2}{dx_1} + d_{44}K_{12}(P_1 - P_1^s) = 0 \quad (37)$$

$$C_{11}(\frac{du_1}{dx_1} - (\alpha^t + 1) - G_{11}\frac{d^3u_1}{dx_1^3} + (d_{11} - f_{11})\frac{dP_1}{dx_1} + e_{12}(P_2 - P_2^s) + f_{11}P_1^s = 0 \quad (38)$$

$$e_{61}(P_1 - P_1^s) + (d_{44} - f_{44})\frac{dP_2}{dx_1} + f_{44}\frac{dP_2^s}{dx_1} = 0 \quad (39)$$

Numerical Simulation

The problem is defined in bidirectional space with one independent spatial variable x_1. The size of simulation cell is taken as twice bigger than the domain wall transition distance. In the case of our simulations,

the domain wall was transiting in 120 nm for P_2 and much smaller for P_1. Thus the simulation cell size was chosen to be 250 nm to guarantee that the boundary conditions will not induce any artificial effect. All boundary conditions in terms of strain are given in both direction x_1 and x_2 to accommodate the spontaneous strain geometrical constraint. Equations 32-39 are discretized through finite differences on a 2500 grid with a constant grid size $\Delta x = 0.1$ nm. The grid size was chosen small enough to provide good resolution in order to allow a better observation of the transition phenomena. All variable are assumed to be zero in the start of the simulation then the strain at $\pm\infty$ is imposed to be equal to the spontaneous strains. Equations 32-35 are explicitly integrated from time t^n to $t^{n+1} = t^n + \Delta t$ to compute the new value for polarization and strain.

Equations 19-30 are only used when there are defects in the material. In the case of defects, the space charge is also integrated explicitly in parallel to the strain and the polarization. The gradient flow method is also described in much reference [14,15]. The convergence of the method is slow especially when the calculation becomes close to the final solution. The parameters chosen were slightly costly in terms of computation resource showever, the results were guaranteed to converge [17-20]. The numerical parameters used are given in Table 1.

Results and Discussion

180° domain wall in perfect Barium Titanate crystal

Figure 4 presents the variation of the normal polarization P_1 and the parallel polarization P_2 across the domain wall. Both polarizations are normalized with respect to the spontaneous polarization magnitude P_0. The Normal polarization P_1 is small compared to the polarization P_2 but it is not zero as it was always assumed. Similar results were found by Yudin et al. [8] and Gu et al. [21], where they found a polarization with a 2 order of magnitude smaller then P_2. The existence of the non-zero polarization induced an electric field around the domain wall with its potential shown in Figure 5. The effect of this polarization is clear in the Figure 6 where the induced electric field causes further distortion of the structure. The strain variation shows the response of the material due to the force exerted by the non-zero polarization.

Parameters	Values	Ref
a_1 (Nm²/C²)	6.6×10^5(T -110)	[17]
a_2 (Nm²/C²)	1.44×10^7(T -175)	[17]
a_3 (Nm²/C²)	3.94×10^9	[17]
a_4 (Nm²/C²)	3.96×10^{10}	[17]
a_5 (Nm²/C²)	2.39×10^{14}	[17]
a_0 (Nm²/C²)	10^{-7}	
c_{11} (N/m²)	275×10^9	[18]
c_{12} (N/m²)	179×10^9	[18]
f_{11} (C/m)	0.35×10^{-9}	[19]
f_{12} (C/m)	5×10^{-6}	[20]
e_{12} (C/N)	-34.5	[22]
e_{22} (C/N)	85.6	[22]
e_{61} (C/N)	392	[22]
E_c (eV)	-3.6	[7]
E_v (eV)	-6.6	[7]
E_d (eV)	-4.0	[7]
N_c;N_v (m^{-3})	10^{24}	[7]
K_1 (1=(eV ms))	10^{13}	[7]
K_2 (1=(eV ms))	10^{11}	[7]
k_1 (s^{-1})	10^{11}	[7]
k_2; k_3 (s^{-1})	10^8	[7]
k_4 ($m^{-2}s^{-1}$)	10^{24}	[7]

Table 1: Material properties.

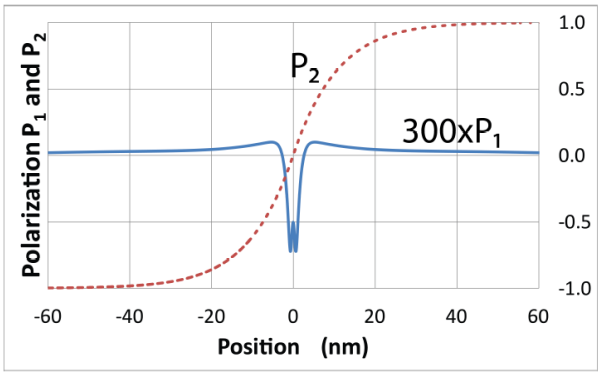

Figure 4: Variation of the polarization P1 and P2 across the 180°domain wall in a perfect crystal.

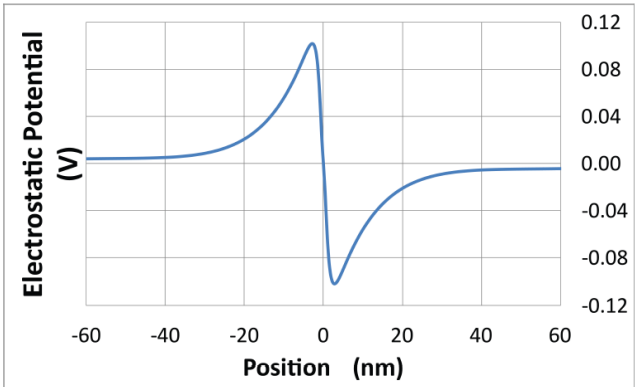

Figure 5: Variation of electrostatic potential Φ across the 180° domain wall in a perfect crystal.

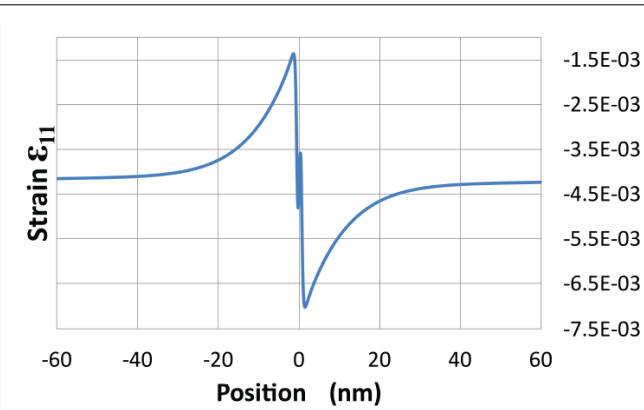

Figure 6: Variation of strain ϵ_{11} across the 180° domain wall in a perfect crystal.

180° domain wall in oxygen vacancy doped Barium Titanate crystal

In this section, we check the effect of exoelectricity on the defects interaction with the domain wall. The typical values of doping in Barium Titanate ranges from 10 to 1000 ppm corresponding to value of

Nd=10^{24}-10^{26} m^{-3}. In this work, we take Nd equal to 10^{24} m^{-3}. The platinum electrode has a work function Φ_e=5.3 eV. Figure 6 shows the variation of polarization across the domain wall. The introduction of defects into the material has no apparent effect on the polarization. The polarization magnitude remains the same as well as the geometrical distortion of the structure. As illustrated in Figure 7, the electrostatic potential shows an average rise compared to the perfect crystal although the electric field remains the same. The total number of ionized donors varies with the electrostatic potential. Figure 8 presents the variation of the ionized donors distribution across the domain wall. At room temperature, the majority of the ionized donors are diffused to the right side of the domain wall. The defects distribution profile shown in this Figure 7 is normalized with respect to the total number of donors in the material. The diffusion of the ionized donors in the domain wall leads to the pinning of the domain wall. In fact, the electrons freed from the ionized donors are swept by the electrostatic potential and they get attracted to the high potential level. The mobile ionized donors are attracted to the potential with low level [22]. The energy required for domain wall motion becomes higher due to the required energy to counter the new electric field created by the distribution of the ionized donors near the domain wall. Xiao et al. [23] studied the interaction between domain walls and oxygen vacancies in tetragonal Barium Tianate. The authors found that the 180° domain has no effect on oxygen vacancy distribution however for the 90° domain wall, the result was similar to what we found in this paper. Yang et al. [24] presented an experimental

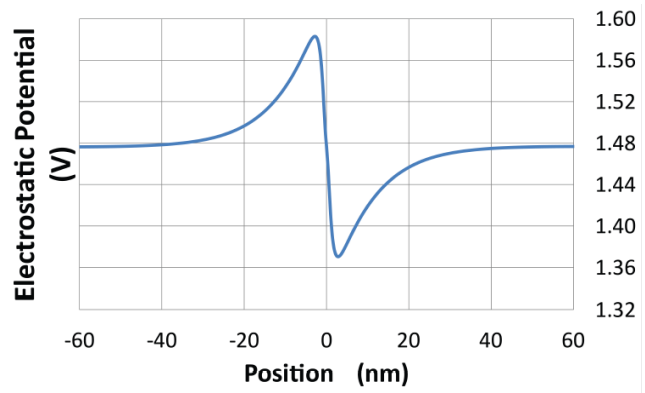

Figure 7: Variation of electrostatic potential Φ across the 180° domain wall in a doped crystal.

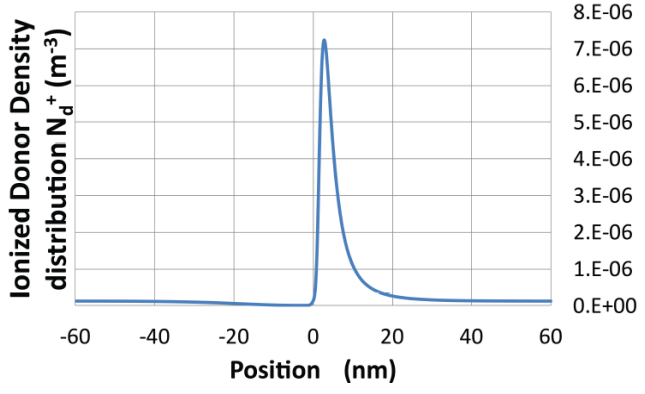

Figure 8: Variation of ionized donor's distribution N_d^+ across the 180° domain wall in a doped crystal.

study of domain wall pinning where they showed that a 180° domain wall can get pinned to defects and impurities in the material which can stop the motion of the domain wall. This behavior is analogous to the electron behavior in high injection of carriers in a PN junction of a semiconductor (such as diode); where it causes to violate one of the approximations made in the derivation of the ideal characteristics, namely that the majority carrier density equals the thermal equilibrium value. One can observe that the majority carrier (electron) density increases beyond the doping density and tracks the minority carrier (hole) density in an extended region away from the junction. High injection of carriers causes to violate one of the approximations made in the derivation of the ideal diode characteristics, namely that the majority carrier density equals the thermal equilibrium value. Excess carriers will dominate the electron and hole concentration. The carrier concentrations decay due to recombination as we move away from the depletion region. A similar behavior was observed in metal-semiconductor contacts for which a synthesis of the thermionic-emission and diffusion approaches has been proposed by Crowell et al. [25] that is derived from the boundary condition of a thermionic recombination velocity near the metal-semiconductor interface [26].

Conclusions

In this work, we presented a new theory for a ferroelectric material which takes into consideration the flexoelectric coupling between the polarization and the strain gradient. We showed that the 180° domain wall has mixed character of Ising and Bloch type. The magnitude of the normal polarization was found to be small compared to the spontaneous polarization. However the mixed character of the domain wall induced a new interaction with defects distribution. It was shown from this analysis that oxygen vacancies are attracted to the domain wall which can pin it and change the piezoelectric properties of the ferroelectric materials. Different parameters are used in this study and although the numerical results were carried only for tetragonal Barium Titanate, the results remain valid for all ferroelectric materials, though, the effect can be either negligible or it can be more important.

References

1. Haun MJ (1988) The Pennsylvania State University.
2. Ghosh D, Sakata A, Carter J, Thomas PA, Han H (2013) Domain wall displacement is the origin of superior permittivity and piezoelectricity in batio$_3$ at intermediate grain sizes. Adv Funct Mater 24: 885-896.
3. Huang XR, Hu XB, Jiang SS, Feng D (1997) Theoretical model of 180° domain-wall structures and their transformation in ferroelectric perovskites. Phys Rev B 55: 5534.
4. Lee D, Behera RK, Wu P, Xu H, Li YL (2009) Mixed bloch-neel-ising character of 180° ferroelectric domain walls. Phys Rev B 80: 060102.
5. Dayal K, Bhattacharya K (2007) A real-space non-local phase field model of ferroelectric domain patterns in complex geometries. Acta Mater 55: 1907.
6. Padilla J, Zhong W, Vanderbilt D (1996) First-principles investigation of 180° domain walls in batio. Phys Rev B 53: 5969.
7. Suryanarayana P, Bhattacharya K (2012) Evolution of polarization and space charges in semiconducting ferroelectrics. J Appl Phys 111: 034109.
8. Yudin PV, Tagantsev AK, Eliseev EA, Morozovska AN, Setter N (2012) Bichiral structure of ferroelectric domain walls driven by flexoelectricity. Phys Rev B 86: 134102.
9. Cao W, Cross LE (1991) Theory of tetragonal twin structures in ferroelectric perovskites with a first- order phase transition. Phys Rev B 44: 5-12.
10. Majdoub MS, Sharma P, Cagin T (2008) Enhanced size-dependent piezoelectricity and elasticity in nanostructures due to the flexoelectric effect. Physical Review B 77: 125424.
11. Majdoub MS, Sharma P, Cagin T (2008) Dramatic enhancement in energy

harvesting for a narrow range of dimensions in piezoelectric nanostructures. Physical Review B 78: 121407.

12. Mindlin RD, Eshel NN (1968) On first strain-gradient theories in linear elasticity. Int J Solids Struct 4: 109-124.
13. Zhang W, Bhattacharya K(2005) A computational model of ferroelectric domains Part I: model formulation and domain switching. Acta Material 53: 185-198.
14. Behrman W (1998) An efficient gradient flow method for unconstrained optimization. Stanford University, Stanford, CA, USA.
15. Andrei N (2004) Gradient flow algorithm for unconstrained optimization. ICI Technical Report.
16. Burcsu E, Ravichandran G, Bhattacharya K (2004) Large electrostrictive actuation of barium titanate single crystals. J Mech Phys Solids 52: 823-846.
17. El-Naggar M, Dayal K, Goodwin DG, Bhattacharya K (2006) Graded ferroelectric capacitors with robust temperature characteristics. J App Phys 100: 114115.
18. Freire JD, Katiyar RS (1988) Lattice dynamics of crystals with tetragonal batio$_3$ structure. Phys Rev B 37: 2074-2085.
19. Hong J, Catalan G, Scott JF, Artacho E (2010) The flexoelectricity of barium and strontium titanates from first principles. J Phys Condens Matter 22: 112201.
20. Ma W, Cross LE (2006) Flexoelectricity of barium titanate. Journal of Appl Phys Lett 88: 232902.
21. Gu Y, Li M, Morozovska AN, Wang Y, Eliseev EA, et al. (2014) Flexo-electricity and ferroelectric domain wall structures: Phase-eld modeling and DFT calculations. Phys Rev B 89: 174111.
22. Berlincourt D, Jaffe H (1958) Elastic and piezoelectric coefficients of single-crystal barium titanate. Phys Rev 111: 143-148.
23. Xiao Y, Shenoy VB, Bhattacharya K (2005) Depletion layers and domain walls in semiconducting ferroelectric thin films. Phys Rev Lett 95: 247603.
24. Yang TJ, Gopalan V, Swart PJ, Mohideen U (1999) Direct observation of pinning and bowing of a single ferroelectric domain wall. Phys Rev Lett 82: 4106.
25. Crowell CR, Sze SM (1966) Current transport in metal-semiconductor barriers. Solid-State Electronics 9: 1035-1048.
26. Sze SM, Ng KK (2007) Physics of semiconductor devices. 3rd Edn. John Wiley and Sons, Inc, USA.